

INFLATED SHEET FLOWS AND THE ORIGIN OF BULBOUS SQUEEZE-UPS

GRADY D. OLSON, Macalester College

Research Advisor: Karl R. Wirth

INTRODUCTION

In the far north of Iceland, at the Krafla central volcano lies a lunar landscape. Hundreds of acres of basaltic lava are frozen in place surrounding the fissures and vents that erupted as recently as 1984. This most recent eruptive event, which likely formed the northern flow field, was observed and is summarized by Harris et al. (2000): "Eruption from an 8.5 km long fissure segment, with activity decreasing within a few hours, but increasing again on September 9 to build a 24 km² flow field." This primary account offers potential insight regarding the style of the eruption that formed the northern flow field and the many unusual features it contains (Fig. 1 A-F), the specifics of which are the focus of this study.

Interspersed amongst more commonly recognized lava flow features are unusual morphologies related to late-stage cooling and flow inflation at several locations. One example is bulbous squeeze-ups associated with pull-apart features (Fig. 1D) in shield-type pahoehoe. These structures have not yet been described in the literature, and have only recently been discovered as well in the Kamakaia Hill flow area, a compound flow field in Hawaii (Rick Hazlett, pers. comm., 2016).

The purpose of this study is to determine the conditions of eruption leading to the formation of three of the unusual flow features observed in the field: bulbous squeeze-ups, elongate squeeze-ups, and jumbled pahoehoe plates. At present it is hypothesized the fissure-fed northern Krafla basalt lava field evolved in discrete pulses on a nearly horizontal slope. These factors contributed in critical ways to develop the unusual features described in this study.

If so, it is possible subtle differences in the lava cooling and flow emplacement history of the three types of features sampled (pahoehoe plates, and bulbous and elongate squeeze-ups) may be recorded in whole rock and mineral textures, associations, and compositions. Field based research, petrographic investigation, and geochemical analysis serve to constrain the sequence, rate, and conditions of formation of bulbous, as well as elongate, squeeze-ups (Fig. 1E) and more generally the surrounding flow field.

INFLATED FLOWS

Inflated sheet flows of basaltic lava, such as the one studied at Krafla, form during long lived eruptions with sustained lava input. This inflation is a result of the rapid chilling of the outermost layer of lava constituting the leading edge of the propagating sheet flow, which acts (similarly to a balloon) to retain incoming lava and form pahoehoe toes at the flow front (Hon, 1994). The formation of a breakout flow lobe (breakout) is the result of plastic deformation in response to internal pressure. On gentle slopes (less than two degrees, and almost always less than one degree) these breakouts commonly coalesce with neighboring breakouts to form a complex flow structure under a cooled upper crust (Hon, 1994). Fractures on this upper crust are formed as a result of deformation associated with areas of pre-existing topography, the uplift of thicker, brittle crust via inflation, and cooling of the upper crust. Brittle fractures propagating into the viscoelastic interior of the flow can be associated with the extrusion of relatively viscous liquid lava from the flow

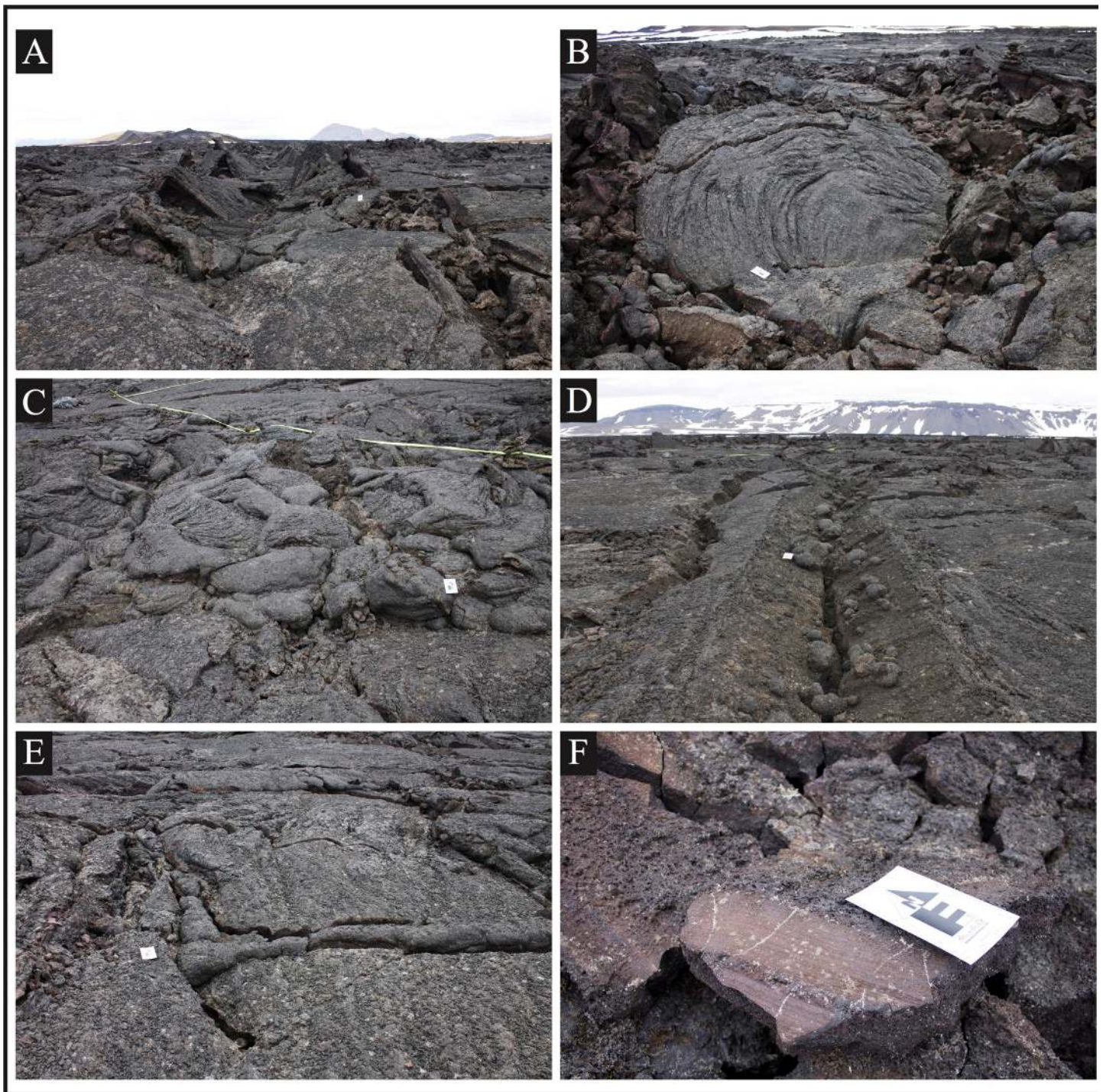


Figure 1. Characteristic features observed in the northern Krafla flow field. Scale included in images is ~20 cm. A) Linear bands of buckled and folded pahoehoe, formed as a result of compressional forces after the upper flow surface was solidified. B) Large, jumbled plate of pahoehoe. C) Complex lava breakout flow features. D) Center of frame: linear pull-apart feature (plastic regime) lined with bulbous squeeze-ups. Left of frame: brittle crack (brittle regime) running parallel to pull-apart feature. E) Elongate squeeze-up feature with 90-degree bend, or kink. F) Underside of extruded lava showing grooves, or striae.

interior. These extrusions are referred to as squeeze-ups, and they occur along the length of the fracture reaching into the liquid lava core. Squeeze-ups vary in geometry (ranging from bulbous to elongate), and it appears that in some circumstances they form more “passively”, forced up solely by the weight of the upper crust. Alternatively, it seems, squeeze-ups form by more “active” processes, in which case the input of liquid lava to the flow causes an increase in pressure and an active extrusion of lava through cracks in the upper surface that reach into the liquid core.

FIELD OBSERVATIONS

The relationships between bulbous and elongate squeeze-ups, as well as the jumbled plates of pahoehoe comprising the northern flow field at Krafla were documented. In particular, the occurrence of bulbous squeeze-ups and associated pull-apart features were investigated.

The northern flow field of Krafla is directly to the west of a North-South trending major fissure feature emanating from the west of Leirhnjúkur Hill at Krafla. It is roughly 1.5 kilometers to the north of Leirhnjúkur Hill and encompasses an area measuring approximately 0.5 by 0.5 km. Centered around the highest concentration of flow features of interest within the northern flow field a sampling grid was created (an area measuring approximately 64 m²). The range of features that make this particular area useful for study are: the co-occurrence of bulbous and elongate squeeze-ups, jumbled pahoehoe plates, and the presence of a variety of features associated with flow inflation (tube fed pahoehoe, very low slope, jumbled sheet flow field with little relief in which broken plates show displacement).

Evidence of compression is observable in folded and buckled areas of the upper crust, as well as extrusion structures (grooves, or striae) on the underside of segments of the upper crust (Fig. 1F) that were thrust on top of nearby solid crust while the basal portion of the overthrust crust was still plastic (Nichols, 1939). Some evidence of shearing exists in grooved and gouged fracture walls. Both brittle and plastic structures occur (Fig. 1D) in places where stresses caused the platy lava crust to fracture (likely during

cooling) or pull apart and separate while the core of the sheet flow was not yet solidified and at least partially molten. At Krafla these interactions somewhat resemble plate tectonics, as has been observed on the surface of lava lakes such as Mauna Ulu, Kupaianaha, and Erta Ale (Duffield, 1972; Harris et al, 2005).

Commonly in the northern flow field where pull-apart features are observed, so too are bulbous squeeze-ups. The pull-apart features on which bulbous squeeze-ups form are consistently v-shaped (Fig. 1D). This geometry indicates the pull-aparts form only where lava can still flow toward the axis of the rift feature after the upper crust has pulled apart. The bulbous squeeze-ups likely are of a comparatively high viscosity upon extrusion. It is this viscosity which allows the bulbous squeeze-up to retain their shape, for if they were able to flow readily they could not retain their bulb-like shape.

Late stage degassing of the inflated sheet flow may play an important role in the geometry of the bulbous squeeze-ups. This late stage degassing could be related to a phenomenon known as second boiling, in which bubbles form in the lava as it is emplaced, during crystallization (Self et al., 1996). The occurrence of this phenomenon could lead to higher viscosity in the lava that forms bulbous squeeze-ups. Because viscosity has a well understood relationship with factors such as vesicularity and crystallinity, these properties were investigated using petrographic microscopy.

PETROGRAPHIC INVESTIGATION

With the conditions of emplacement and flow history in mind, the principal goals of petrographic investigation were to:

1. Characterize the texture and mineral composition of plagioclase (phenocrysts and microlites), olivine, and pyroxene, and
2. To determine what trends, if any, in textural properties and mineral compositions across features exist (i.e. increasing crystallinity towards the interior of the flow).

In order to characterize and compare each type of feature in terms of composition and overall texture (vesicularity, crystallinity, mineral textures) thin sections of each type of sample were prepared.

Each flow feature sampled displays variability in physical properties from the flow top to the flow interior on the macroscopic level. Accordingly, each sample was divided into a “rim” and “core”, with the division occurring at the most pronounced, abrupt change in texture (Fig. 2). Thin sections above, below, and spanning this transition were prepared for each feature when enough material was present (in some cases only two thin sections were prepared).

Changes in petrographic properties within a given feature were consistent across all of the flow features sampled. Petrographic and scanning electron microscopy (SEM) indicate consistently high crystallinity (~50% of rock material) and vesicularity (~40% in terms of overall area). Optical investigation suggests rock textures do not change between bulbous squeeze-ups, elongate squeeze-ups, and plates; rather they change as a function of distance from flow top (lava-atmosphere interface). Thus, the textural changes observed are consistent across all flow features analyzed.

All of the flow features of interest are characterized by a pilotaxitic to intergranular texture consisting of laths of plagioclase microlites (typically $10 \times 50 \mu\text{m}$) with few (~1%) normally (and uncommonly multiple even oscillatory) zoned plagioclase phenocrysts (up to $0.5 \times 2 \text{ mm}$) (Fig. 3A, B). Interstitial augite with dendritic textures are common throughout (Fig. 3C), and appear to regularly nucleate on plagioclase, possibly due to localized enrichment in mafic mineral forming constituents, as plagioclase depletes Si, Al, and Ca (Winter, 2012). The presence of olivine (<5%, typically $20 \times 40 \mu\text{m}$) was confirmed with SEM (Fig. 3B). Ilmenite and titanium rich magnetite are common and exist in interstitial space; they are dendritic in habit (Fig. 3D). This phenomenon merits further study, as the growth history of dendritic magnetite and ilmenite has been investigated and constrained in terms of relative timing and temperature of crystallization (Kretz, 2003).

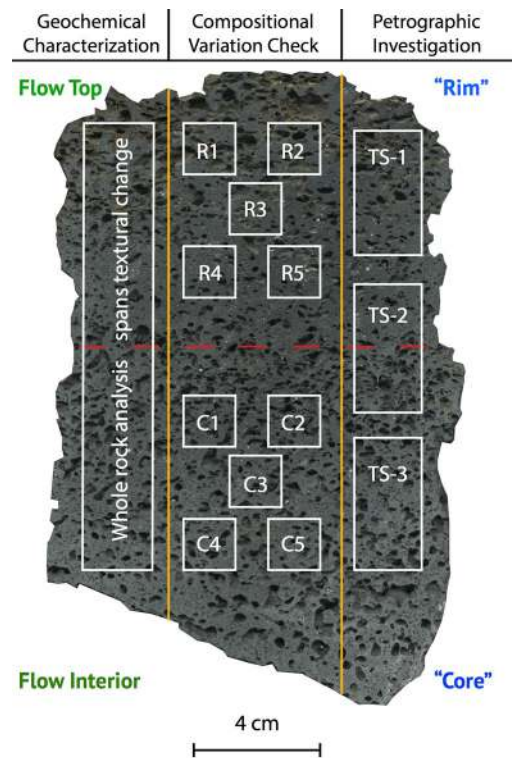


Figure 2. Visual representation of sample preparation for geochemical and petrographic investigation. Green labels denote orientation of sample, and blue labels designate naming scheme. Observed textural change (in vesicularity) is marked by dotted red line while yellow lines separate the sample in terms of the purpose of sample preparation. Geochemical characterization utilized rock material spanning the textural change. Compositional variation checks consisted of five samples from the core and rim (i.e. C1-C5). Petrographic investigation was comprised of 2-3 thin sections spanning the textural change.

Initial investigation of the compositions of minerals analyzed within and across features reveals that the mineral chemistry within a given type of mineral appears consistent throughout all features of interest (Table 1). Statistical comparisons suggest significant variation within individual features (Table 1). Because of this, statistical comparisons were made using mineral compositions averaged across an entire feature.

GEOCHEMICAL ANALYSIS

Whole rock major and trace element concentrations are highly sensitive to differences in proportions of crystals and glass in a rock, and as such whole rock samples of bulbous, and elongate squeeze-ups, and plates were investigated geochemically.

Table 1. Compositional results and statistical comparisons of olivines, plagioclase phenocrysts, plagioclase microlites, and pyroxenes (augites) within and across pahoehoe plates, bulbous squeeze-ups, and elongate squeeze-ups. Sample size (n =) and end member type (i.e. "An" for anorthoclase #) are included for each mineral composition analysis. Statistical comparisons are color coded as the product of the two compositional results (i.e. "Bulbous squeeze-up vs plate" has a purple background because the "Bulbous squeeze-up" and Plate" compositional values have red and blue backgrounds, respectively. Additionally, individual P-value results in statistical comparisons are colored such that significant differences in composition (P-value < 0.05) are red, nearly significant differences in composition (0.05 < P-value < 0.1) are yellow, and non-significant differences in composition (P-value > 0.1) are red.

Internal Compositional Comparison												
Bulbous Squeeze-up Rim	n = 5	Olivine	2 σ Error	n = 5	Plag. Phenocryst	2 σ Error	n = 5	Plag. Microlite	2 σ Error	n = 5	Augite	2 σ Error
	Te	0.40	0.17	An	67.70	3.34	An	67.78	3.44	Wo	33.79	5.33
	Fo	67.88	4.19	Ab	31.51	3.52	Ab	31.65	3.43	En	46.62	4.94
	Fa	31.12	4.12	Or	0.79	0.64	Or	0.56	0.65	Fs	19.58	5.33
Bulbous Squeeze-up Core	n = 5	Olivine	2 σ Error	n = 5	Plag. Phenocryst	2 σ Error	n = 5	Plag. Microlite	2 σ Error	n = 5	Augite	2 σ Error
	Te	0.40	0.10	An	65.75	4.67	An	65.27	2.98	Wo	35.45	4.07
	Fo	67.25	3.64	Ab	33.07	4.30	Ab	33.40	2.69	En	43.87	5.24
	Fa	31.67	3.40	Or	1.18	0.94	Or	1.34	0.96	Fs	20.69	8.96
Internal Statistical Comparison												
Bulbous Squeeze-up Rim vs Core	Olivine	P-value		Plag. Phenocryst	P-value		Plag. Microlite	P-value		Augite	Augite	
	Te	0.77		An	0.27		An	0.09		Wo	0.41	
		0.65		Ab	0.35		Ab	0.20		En	0.20	
		0.71		Or	0.14		Or	0.04		Fs	0.70	
Compositional Comparison Across Features												
Bulbous Squeeze-up	n = 10	Olivine	2 σ Error	n = 10	Plag. Phenocryst	2 σ Error	n = 10	Plag. Microlite	2 σ Error	n = 10	Augite	2 σ Error
	Te	0.40	0.15	An	66.72	4.51	An	65.27	4.05	Wo	34.71	4.95
	Fo	67.64	4.04	Ab	32.29	4.23	Ab	33.40	3.50	En	45.09	5.80
	Fa	31.33	3.91	Or	0.98	0.90	Or	1.34	1.13	Fs	20.20	7.64
Elongate Squeeze-up	n = 3	Olivine	2 σ Error	n = 2	Plag. Phenocryst	2 σ Error	n = 3	Plag. Microlite	2 σ Error	n = 4	Augite	2 σ Error
	Te	0.39	0.11	An	66.69	4.88	An	65.42	4.72	Wo	30.60	2.54
	Fo	65.97	4.91	Ab	32.40	4.11	Ab	33.65	4.22	En	45.20	9.21
	Fa	32.96	4.58	Or	0.91	0.77	Or	0.94	0.53	Fs	24.19	7.51
Plate	n = 10	Olivine	2 σ Error	n = 10	Plag. Phenocryst	2 σ Error	n = 10	Plag. Microlite	2 σ Error	n = 7	Augite	2 σ Error
	Te	0.44	0.22	An	67.02	2.50	An	65.94	7.04	Wo	31.41	6.96
	Fo	64.58	5.76	Ab	32.50	2.51	Ab	33.48	6.62	En	45.96	6.42
	Fa	34.29	5.41	Or	0.47	0.26	Or	0.58	0.57	Fs	22.63	6.17
Statistical Comparison Across Features												
Bulbous vs Elongate Squeeze-up	Olivine	P-value		Plag. Phenocryst	P-value		Plag. Microlite	P-value		Augite	P-value	
	Te	0.81		An	0.99		An	0.63		Wo	0.00	
	Fo	0.45		Ab	0.97		Ab	0.58		En	0.97	
	Fa	0.43		Or	0.88		Or	0.84		Fs	0.17	
Bulbous Squeeze-up vs Plate	Olivine	P-value		Plag. Phenocryst	P-value		Plag. Microlite	P-value		Augite	P-value	
	Te	0.41		An	0.76		An	0.75		Wo	0.07	
	Fo	0.02		Ab	0.81		Ab	0.51		En	0.61	
	Fa	0.02		Or	0.01		Or	0.09		Fs	0.21	
Elongate Squeeze-up vs Plate	Olivine	P-value		Plag. Phenocryst	P-value		Plag. Microlite	P-value		Augite	P-value	
	Te	0.39		An	0.91		An	0.81		Wo	0.63	
	Fo	0.53		Ab	0.97		Ab	0.93		En	0.81	
	Fa	0.53		Or	0.46		Or	0.19		Fs	0.56	

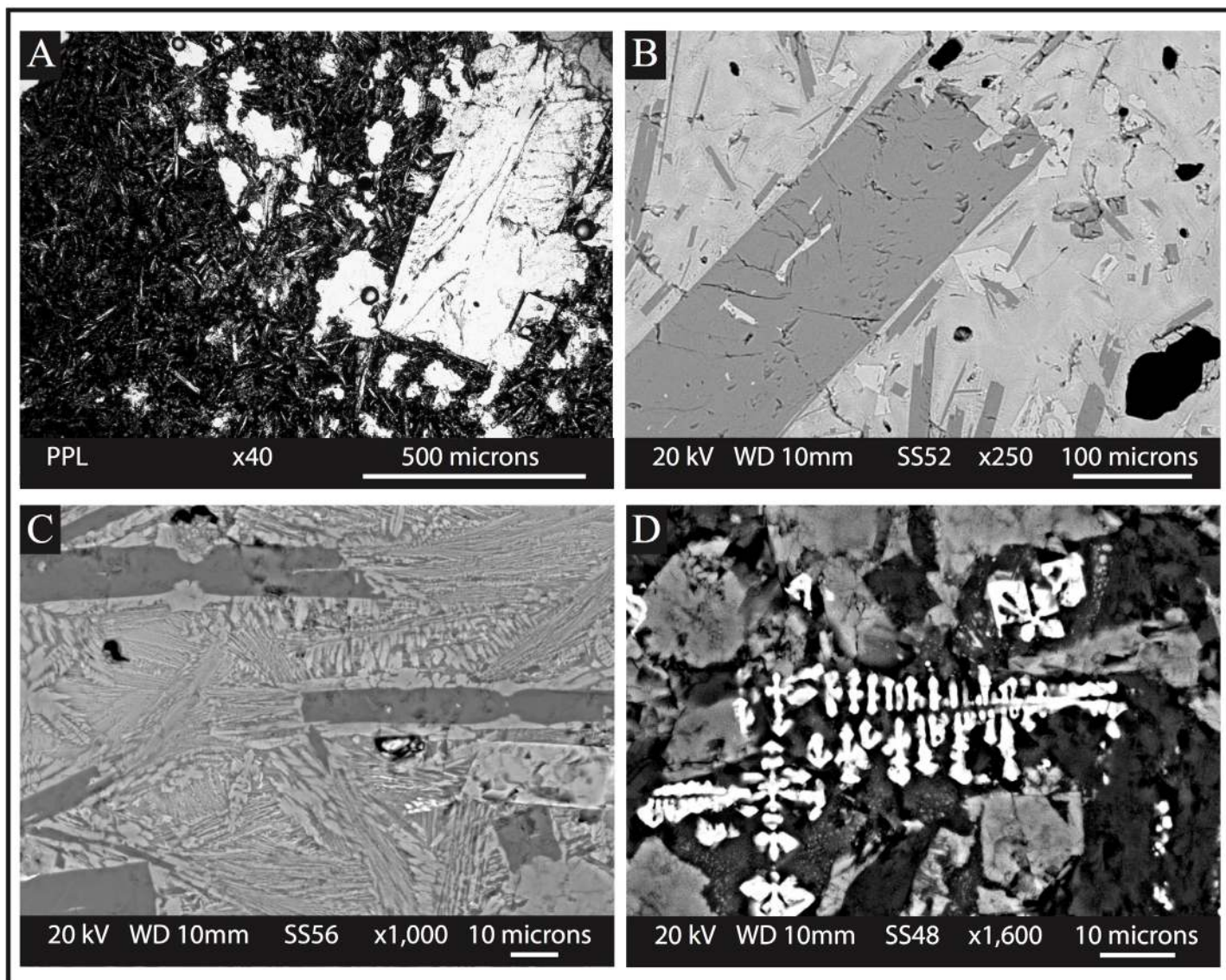


Figure 3. Images from petrographic and scanning electron microscopes showing characteristic minerals and textures. A) Plane polarized light (PPL) image showing typical thin section view of matrix and plagioclase phenocryst. B) Back scatter electron (BSE) image showing typical textures and relationships between matrix (variable in color), plagioclase (microlites and phenocrysts, darkest color values) and olivine crystal (brightest crystals, approaching euhedral habit). C) Close up BSE image showing skeletal plagioclase microlites with overgrown augite, and interstitial dendritic augite. D) Close up BSE image of dendritic ilmenite and titanium rich magnetite.

Instrumental error, the error of sample preparation and analysis, as well as the natural variation inherent to each sample prepared were quantified (Table 2), where geochemical sample preparation follows the methods outlined in Vervoort et. al. (2007). A comparison of multiple samples ($n = 5$) from the “core” and “rim” was conducted to discover that major and trace element composition vary within a single feature. Accordingly, X-Ray Fluorescence Spectrometer (XRF) samples used to characterize each feature were prepared using enough material from the sample collected in the field such that bulk

elemental composition of the entire sample analyzed was determined accurately (Fig. 2).

Compositional comparisons were made only for elements with a total relative error of less than 10% (with the exception of barium which had an error only slightly above 10%, see Table 2). Statistical comparisons of the compositions of groups of samples (grouped by feature type) were made using Cohen’s D (d), a measure of practical significance, or effect size (Equation 1).

$$d = \frac{\text{Mean}_1 - \text{Mean}_2}{\left(\frac{\sqrt{SD_1^2 + SD_2^2}}{2} \right)}$$

(1)

The results of these comparisons are seen in Figure 4, for major and trace elements. In nearly all circumstances, with 95% confidence, there is no significant difference in the chemical compositions of these features. Two of the six elements that stand out (Fe_2O_3 and Cu) are possibly a result of contamination (saw blade, rock crusher) during sample preparation. Other elements such as MnO, Na_2O , and P_2O_5 have relatively high effect sizes, which is possibly a result of relatively low concentrations which fall near the instrumental limit of quantification (Table 2). Finally, Sr appears to vary significantly between bulbous and elongate squeeze-ups, a result which has no understood implication with regard to the relative cooling histories of these features.

DISCUSSION

With the data currently available it is uncertain if the observed variations in mineral compositions represent meaningful differences, or are simply a result of a limited sample size. The lack of trends in mineral compositions across bulbous squeeze-ups, elongate squeeze-ups, and plates indicates that these three features are indiscernible in terms of mineral geochemistry. Further study with an increased sample size could prove otherwise, as it is plausible, for example, that the composition of plagioclase microlites may be sensitive to flow fractionation across features.

Additionally, changes in macroscopic textural properties do not co-occur with changes in composition. In other words, the quenched lava surface is of the same composition as the more slowly cooling flow interior (on the scale sampled in this study). Investigations of systematic variation in vesicularity and crystallinity on a larger scale are recommended, as previous work (Teasdale and Szymanski, 2015) has demonstrated significant changes in groundmass crystallinity (crystal size and

crystals per unit area) are a function of cooling rate and distance from vent, which could ultimately prove useful in constraining the conditions of formation of unusual features in the northern flow field at Krafla. In-depth analysis of vesicle content (size and frequency) across features could also support or refute the notion that a second boiling event may be responsible for an increased viscosity in bulbous squeeze-ups.

Geochemical and petrographic analyses of samples from Krafla do not demonstrate significant differences between bulbous squeeze-ups, elongate squeeze-ups, and the surrounding pahoehoe plates. This indicates the spectrum of flow morphologies observed at Krafla all formed from one homogenous magma, and that this magma did not fractionate. Consequently, the observed association between bulbous squeeze-ups and pull-apart ridges indicates the unusual timing and rate of emplacement were the primary drivers of the formation of these squeeze-up features. With this in mind, there are several scenarios in which the flow field might have formed.

It is feasible that the bulbous and elongate squeeze-ups, as well as the jumbled pahoehoe plates, all formed practically contemporaneously, and the flow field was fully emplaced shortly after erupting (hours-days, as opposed to weeks-months).

Alternatively, the flow field took longer to form, and was the result of a pulsed eruptive event. In this scenario, the primary input of lava that cooled relatively early would have been responsible for the formation of the majority of pahoehoe plates observed in the northern flow field. A later pulse of lava (of the same composition as the first pulse) could flow from the vent, inflating the now chilled “primary” flow, acting to transport lava beneath a cooled upper crust. This sub-crustal flow may have acted to shear, collide, and pull apart plates of pahoehoe, and in some circumstances actively extrude lava, creating squeeze-ups in a variety of forms. Additionally, this subcrustal flow may have facilitated the transport of bubbles formed during a second boiling event (related to crystallization) to reach the surface at the pull-apart ridges. Increased vesicularity as a result of second boiling would have the effect of

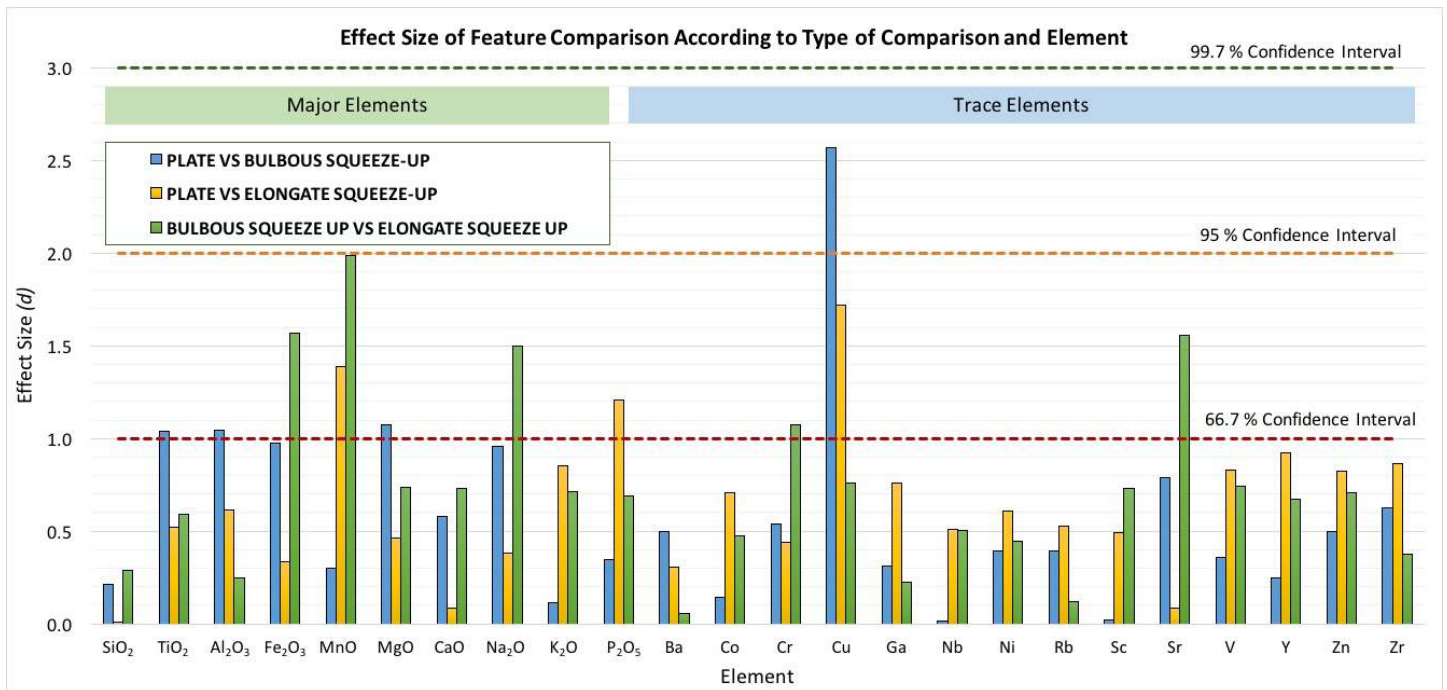


Figure 4. Chart showing effect sizes, or Cohen's D (d) between average elemental concentrations from analyses ($n=5$) of each feature type. Values of d above 1 indicate that the differences in average concentration between features are significant at the 66.7% confidence interval. The 95% and 99.7% confidence intervals correspond to values of d of 2 and 3 (of which there are none).

increasing the overall viscosity, enabling the bulbous squeeze-ups to maintain a nearly-spherical geometry after being extruded. This scenario involving a discontinuous eruptive style is in agreement with the direct observation of a later pulse of activity in the eruption at Krafla summarized by Harris et al. (2000). Ultimately, however, further study of similar flow fields, and observations of inflated sheet flows actively being emplaced are needed to further constrain the most probable scenario in which these squeeze-ups form.

Eventually, the direct observation of the formation of bulbous squeeze-ups will constrain the conditions under which they form. Until then, more detailed studies of the field relations of the northern flow field of Krafla, along with more precise mineral composition investigation across the suite of features there, can serve to constrain the parameters required to form bulbous squeeze-ups. If the manner in which bulbous squeeze-ups form is determined, the identification of this distinctive morphology could be extremely telling of eruptive conditions of past eruptions on earth, as well as on other planets with observable lava flows.

CONCLUSIONS

Unusual manifestations of an inflated basaltic lava flow are found in the northern flow field of the Krafla caldera in northern Iceland. Distinctive bulbous squeeze-ups, the likes of which have not been described in the literature to date, develop on the edges of jumbled pahoehoe plates, and zones of, shearing, compression and extension (pull-apart features). Whole rock geochemical analysis of major and trace element composition indicate that the spectrum of features observed at Krafla are of uniform composition. Mineral compositions across features agree with the whole rock geochemical findings. The range in morphology and association of pahoehoe plates, bulbous and elongate squeeze-ups all indicate a history of discontinuous flow inflation in which sub-crustal flow and possibly second boiling may have taken place. Finally, the jumbled nature of the flow field, with locally high strains, suggests a somewhat violent and possibly pulsed inflation history that occurred on the scale of hours-days.

ACKNOWLEDGEMENTS

Funding for this project was provided by the Keck Geology Consortium. Many thanks to Jeff Karson and Rick Hazlett for making this project possible. Thanks to Bryndis Brandsdóttir for assisting with lodging at Krafla. I am very grateful to Bob Wysocki, as well as Esme Faneuff, Nelson Bandy, Ariel Hampton, Erin Hightower and Trevor Maggart for making the pours at Syracuse possible, and for assisting with every aspect of gathering data for each pour. Thanks to Jeff Thole and Karl Wirth for advising and assisting with data collection at Macalester.

REFERENCES

- Buhrke, V. E., Jenkins, and Smith, 1998, Practical guide for the preparation of specimens for x-ray fluorescence and x-ray diffraction analysis: Wiley-VCH.
- Cashman, K. V., and Kauahikaua, 1997, Reevaluation of vesicle distributions in basaltic lava flows: *Geology*, v. 25.5, p. 419-422.
- Colton, H. S., and Park, 1930 Anosma or squeeze-ups, American Association for the Advancement of Science.
- Duffield, W. A., 1972, A naturally occurring model of global plate tectonics. *Journal of Geophysical Research*: v. 77.14
- Garden, J. R., and Laughlin, A. W., 1974, Petrochemical Variations within the McCartys Basalt Flow, Valencia County, New Mexico: *Geological Society of America Bulletin* 85.9, p. 1479-1484.
- Harris, A. J.L., et al., 2000, Effusion rate trends at Etna and Krafla and their implications for eruptive mechanisms. *Journal of Volcanology and Geothermal Research*: no. 102.3, p. 237-269.
- Harris, A. J.L., Carniel, and Jones, 2005, Identification of variable convective regimes at Erta Ale Lava Lake. *Journal of Volcanology and Geothermal Research*: v. 142.3, p. 207-223.25
- Hon, K., Denlinger, Kauahikaua, and Mackay, 1994, Emplacement and Inflation of Pahoehoe Sheet Flows: Observations and Measurements of Active Lava Flows on Kilauea Volcano, Hawaii. *The Geological Society of America Bulletin*: no. 106.3, Print.
- Karson, J. A., and Wysocki, R. J., 2012, Do-it-yourself lava flows: Science, Art and Education in the Syracuse University Lava Project: *Earth* 57.9, p. 38.
- Keszthelyi, L., and Self, 1998, Some physical requirements for the emplacement of long basaltic lava flows. *Journal of Geophysical Research: Solid Earth (1978–2012)* v. 103.B11, p. 27447-27464.
- Kretz, R., 2003, Dendritic magnetite and ilmenite in 590 Ma Grenville dikes near Otter Lake, Quebec, Canada. *The Canadian Mineralogist*: v. 41.4, p. 1049-1059.
- Lev, E., Karson, J., Spiegelman, M., Wysocki, R., 2012, Investigating lava flow rheology using video analysis and numerical flow models. *Journal of Volcanology and Geothermal Research*: v. 247, p. 62-73.
- Nichols, R. L., 1938, Grooved lava. *The Journal of Geology*: p. 601-614.
- Nichols, R. L., 1939, Surficial banding and shark's-tooth projections in the cracks of basaltic lava. *American Journal of Science*: v. 237.8, p. 188-194.
- Nichols, R. L., 1939, Squeeze-ups. *The Journal of Geology*: p. 421-425.
- Nicholson, H., Latin, D., 1992, Olivine Tholeiites from Krafla, Iceland: Evidence for Variations in melt fraction within a plume: *Journal of Petrology*: v. 33, p. 1105-1124
- Oze, C., and Winter, J.D., 2005, The occurrence, vesiculation, and solidification of dense blue glassy pahoehoe. *Journal of Volcanology and Geothermal Research*: v. 142.3, p. 285-301.
- Pitard, F., 1993, Pierre Gy's sampling theory and sampling practice: heterogeneity, sampling correctness, and statistical process control: Boca Raton, CRC Press.
- Rossi, M. J., 1997, Morphology of the 1984 open-channel lava flow at Krafla volcano, northern Iceland. *Geomorphology*: v. 20.1, p. 95-112.
- Self, S., Finnemore, S., Hon, K., Keszthelyi, L., Long, P., Murphy, M. T., Thordarson, Th., and Walker, G. P. L., 1996, A new model for the emplacement of Columbia River basalts as large, inflated pahoehoe lava flow fields. *Geophysical Research Letters*: no. 23.19, p. 2689-2692.

- Teasdale, R., and Szymanski, 2015, Groundmass Crystallinities of Proximal and Distal Lavas from Cinder Cone, Lassen Volcanic Field. AGU Fall Meeting: Web.
- Vervoort, Wirth, Kennedy, Bryan, Sandland, and Harpp, 2007, The magmatic evolution of the Midcontinent rift: New geochronologic and geochemical evidence from felsic magmatism. *Precambrian Research*: v. 157.1, p. 235-268.
- Winter, J. D., 2010, *Principles of igneous and metamorphic petrology*: v. 2, New York: Prentice Hall.

